

Pacific Northwest National Laboratory

Operated by Battelle for the
U.S. Department of Energy

Retained Gas Sampler Extractor Mixing and Mass Transfer Rate Study: Experimental and Simulation Results

K. P. Recknagle
J. M. Bates
A. Shekarriz

RECEIVED
DEC 17 1997
OSTI

November 1997

19980504 091

DTIC QUALITY INSPECTED 4

Prepared for the U.S. Department of Energy
under Contract DE-AC06-76RLO 1830

DISCLAIMER

This report was prepared as an account of work sponsored by an agency of the United States Government. Neither the United States Government nor any agency thereof, nor Battelle Memorial Institute, nor any of their employees, makes any warranty, express or implied, or assumes any legal liability or responsibility for the accuracy, completeness, or usefulness of any information, apparatus, product, or process disclosed, or represents that its use would not infringe privately owned rights. Reference herein to any specific commercial product, process, or service by trade name, trademark, manufacturer, or otherwise does not necessarily constitute or imply its endorsement, recommendation, or favoring by the United States Government or any agency thereof, or Battelle Memorial Institute. The views and opinions of authors expressed herein do not necessarily state or reflect those of the United States Government or any agency thereof.

PACIFIC NORTHWEST NATIONAL LABORATORY
operated by
BATTELLE
for the
UNITED STATES DEPARTMENT OF ENERGY
under Contract DE-AC06-76RLO 1830

Printed in the United States of America

Available to DOE and DOE contractors from the
Office of Scientific and Technical Information, P.O. Box 62, Oak Ridge, TN 37831;
prices available from (615) 576-8401.

Available to the public from the National Technical Information Service,
U.S. Department of Commerce, 5285 Port Royal Rd., Springfield, VA 22161



This document was printed on recycled paper.

**Retained Gas Sampler Extractor Mixing
and Mass Transfer Rate Study:
Experimental and Simulation Results**

K. P. Recknagle
J. M. Bates
A. Shekarriz

November 1997

DISTRIBUTION OF THIS DOCUMENT IS UNLIMITED *ph*

Prepared for
the U.S. Department of Energy
under Contract DE-AC06-76RLO 1830

MASTER

Pacific Northwest National Laboratory
Richland, Washington 99352

Summary

Research staff at Pacific Northwest National Laboratory conducted experimental testing and computer simulations of the impeller-stirred Retained Gas Sampler (RGS) gas extractor system. This work was performed to verify experimentally the effectiveness of the extractor at mixing viscous fluids of both Newtonian and non-Newtonian rheology representative of Hanford single- and double-shell wastes, respectively. Developing the computational models and validating their results by comparing them with experimental results would enable simulations of the mixing process for a range of fluid properties and mixing speeds.

Five tests were performed with a full-scale, optically transparent model extractor to provide the data needed to compare mixing times for fluid rheology, mixer rotational direction, and mixing speed variation. The computer model was developed and exercised to simulate the tests.

The tests demonstrated that rotational direction of the pitched impeller blades was not as important as fluid rheology in determining mixing time. The Newtonian fluid required at least six hours to mix at the hot cell operating speed of 3 rpm, and the non-Newtonian fluid required at least 46 hours at 3 rpm to become significantly mixed. In the non-Newtonian fluid tests, stagnant regions within the fluid sometimes required days to be fully mixed. Higher-speed (30 rpm) testing showed that the laminar mixing time was correlated to mixing speed. The tests demonstrated that, using the RGS extractor and current procedures, complete mixing of the waste samples in the hot cell should not be expected.

The computer simulation of Newtonian fluid mixing gave results comparable to the tests while simulation of non-Newtonian fluid mixing would require further development. In light of the laboratory test results, detailed parametric analysis of the mixing process was not performed.

Acknowledgments

The authors would like to acknowledge the assistance of Scott Cannon and Dennis Graves of SGN Eurisys Services Corporation for producing the experimental apparatus for this study, Bill Combs (PNNL) for contributing his expertise in the laboratory, and Hank Reid (PNNL) for contributing his expertise in the use of the computer code.

Contents

Summary	iii
Acknowledgments	v
1.0 Introduction	1
2.0 Experimental Method	3
2.1 Apparatus	3
2.2 Fluid Properties	5
2.3 Test Matrix	5
2.4 Experimental Test Results	6
2.4.1 Newtonian Fluid	7
2.4.2 Non-Newtonian Fluid	7
3.0 Computational Method	15
3.1 CFX-F3D Model	15
3.2 Computations	16
3.2.1 Newtonian Fluid Simulations	16
3.2.2 Non-Newtonian Fluid Simulations	17
4.0 Conclusions	19
5.0 References	21

Figures

1.1 Dimensionless Mixing Time Versus Reynolds Number for Impeller Mixing	2
2.1 Elevation and Plan Views of Mixer Apparatus	4
2.2 Schematic of Experimental Apparatus	4
2.3 Rheogram for Working Fluid	6
2.4 Newtonian Mixing (3 rpm, up pressure, glycerin and fluorescent dye)	8
2.5 Newtonian Mixing (3 rpm, down pressure, glycerin and fluorescent dye)	9
2.6 Non-Newtonian Mixing (3 rpm, up pressure, Carbopol and fluorescent dye)	11
2.7 Non-Newtonian Mixing (3 rpm, down pressure, Carbopol and fluorescent dye)	12
2.8 Non-Newtonian Mixing (30 rpm, down pressure, Carbopol and fluorescent dye)	13
3.1 Elevation and Plan Views of Mixer Model Domain	15
3.2 Tracer in Glycerin after 400 Seconds of 3-rpm Down-Pressure Mixing (homogeneous multiphase model)	18
3.3 Tracer in Glycerin after 400 Seconds of 3-rpm Down-Pressure Mixing (disperse multiphase model)	18
3.4 Tracer in Carbopol Solution after 400 Seconds of 3-rpm Down-Pressure Mixing (disperse multiphase model)	18
3.5 Tracer in Carbopol Solution after 400 Seconds of 3-rpm Down-Pressure Mixing (disperse multiphase model)	18

Tables

2.1 Extractor Mixing Tests	6
----------------------------------	---

1.0 Introduction

Mixing, or agitation, is an important component of gas extraction in the Retained Gas Sampler (RGS) system. Shekarriz et al. (1997) and Mahoney et al. (1997) are two documents that describe the details of the gas extraction process in the hot cell. Briefly, after sampling, the content of the RGS is extruded into the gas extraction system (extractor) within the hot cell. During the gas extraction process (using a mercury vacuum pump), the sample is agitated with a dual-impeller mixer rotating at 3 rpm. This agitation was assumed necessary to improve the rate of mass transfer of the dissolved gases trapped in the waste sample. Although the mixer is designed to rotate at much higher rates, the rotation rate is constrained by the durability of the motor seals that prevent loss or contamination of RGS gases during gas extraction.

Dislodging the insoluble gas bubbles from the waste sample is not considered to be significantly affected by the mixing rate. During the gas extraction process a low vacuum is drawn on the system. The reduced head space pressure produces a net force on the gas bubbles toward the surface and is thought to provide sufficient mechanism for their release. However, transport of the soluble gases, especially ammonia, may be hindered by the mixing rate of the waste sample in the extractor. Mahoney et al. (1997) discuss some of the inconsistencies observed in the data associated with concentrations of ammonia measured using the current RGS approach. While several explanations may be available for the lack of consistency in the data, the most likely scenario is thought to be poor mixing in the extractor. Indeed, under conditions where the mass transfer is limited by the liquid-side transport, the assumptions used for application of Henry's law for estimating the quantity of ammonia extracted may be in jeopardy.

Mixing time is heavily dependent on the Reynolds number, as was found by Fox and Gex (1956). Figure 1.1 plots the nondimensional mixing time as a function of Reynolds number for Newtonian and non-Newtonian fluids, as determined experimentally by Moo-Young et al. (1972) for a stirred vessel. These results are typical of mixing within a vessel, where, as the Reynolds number approaches zero, the dimensionless mixing time approaches infinity. However, these results also show that a significantly higher mixing rate, somewhat independent of Reynolds number, may be achieved if the flow becomes turbulent. Distelhoff et al. (1997) showed that turbulent mixing times can be on the order of seconds in impeller-stirred tanks.

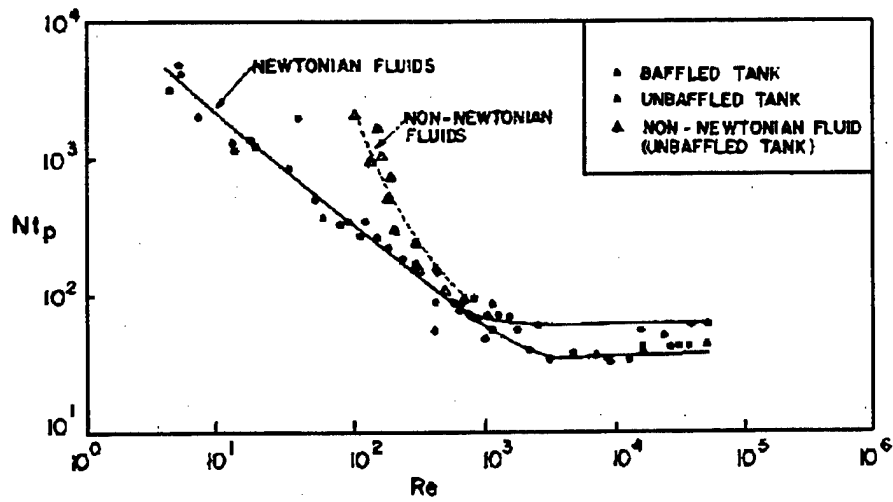


Figure 1.1. Dimensionless Mixing Time Versus Reynolds Number for Impeller Mixing

Reynolds numbers in the extractor are expected to be small. For a 3-rpm mixing speed, a density of 10^3 kg/m^3 , a container diameter of roughly 10 cm, and viscosities ranging from 10^{-2} to 10^2 Pa-s , the Reynolds number ranges from 0.032 and 320. Thus the flow within the extractor during mixing is laminar (and creeping when fairly viscous sludges are present). Thus, a notably low rate of mixing can be expected for most of the sludge samples taken from various double-shell tanks or saltcake samples taken from single-shell tanks. The presence of shear thinning rheology or yield stress will reduce the rate of mixing even further, as shown in Figure 1.1.

Recently, Bobroff et al. (1997) used nuclear magnetic resonance (NMR) to measure the diffusion coefficient of ammonia as a function of fluid viscosity and packing fraction of solids in a slurry. Their results suggest that as the fluid viscosity increases or when the concentration of solid particles in a packed bed becomes significant, then the diffusivity of ammonia in the mixture is retarded. Thus, in addition to a poor bulk mixing rate, the diffusion-limited mixing suffers from further attenuation in the species diffusivity.

Considering some of the issues discovered so far, it was deemed necessary to investigate further the extent to which mixing within the extractor may be considered poor. We have embarked on experimental as well as computational verification of the mixing rate under conditions in which the fluid is Newtonian and in which the fluid is non-Newtonian. This report presents a summary of our results and observations.

2.0 Experimental Method

This section describes the methodology and results of a series of flow visualization experiments performed in the laboratory at PNNL. The objective of this work was to perform full-scale testing of the extractor mixing process to obtain qualitative information about the effectiveness of the mixing. An optically transparent vessel was used to enable visual observation of the degree of mixing achieved. Viscous Newtonian and non-Newtonian fluids were used as simulants to bound the rheologies of single- and double-shell tank wastes.

2.1 Apparatus

The test apparatus was a full-scale mockup of the actual extractor using project spare parts that included the stepper motor, motor controller, and shaft with impellers. The portion of the mixer that engaged the fluid comprised the impeller shaft and two impellers, each with three variable-pitch, tapered blades. The pitch, averaging about 24° , was oriented such that counter-clockwise motion placed the blades pressure side upward. The lower impeller had a radius of 4.83 cm (1.90 in.). The upper impeller had the blades shortened so the radius was 4.44 cm (1.75 in.) to promote more recirculation within the extractor and to provide clearance for the thermocouple thermowells. Figure 2.1a is a photograph showing the general configuration of the mixer and the difference in impeller blade length.

In place of the 4-in. schedule 40 pipe that houses the actual extractor, a clear Lexan[®] tube of 5.08 cm (2 in.) radius was used enabling flow visualization. A clear Lexan band 0.18 cm (0.07 in.) thick and 1.28 cm (0.5 in.) high was bonded to the lower inside of the housing at the lower impeller level. The Lexan band was added to simulate a sealing ring on the actual extractor. The effect of the band was to decrease the clearance between the lower impeller blade tips and the outer housing wall to 0.76 cm (0.03 in.). The tip clearance of the upper blade was 0.64 cm (0.25 in.). Figure 2.1b gives a plan view of the mixer and shows the difference in blade tip clearance of the upper and lower impellers.

Figure 2.2 is a schematic of the test setup at the camera viewing angle. The speed and direction of mixer rotation was maintained by a motor controller. A laser light source and associated optics were used to produce a laser sheet to illuminate a vertical plane through the Lexan housing and the test fluid. This plane was viewed from a position normal to the plane by a digital video camera, and monitored images were stored to a laser disk.

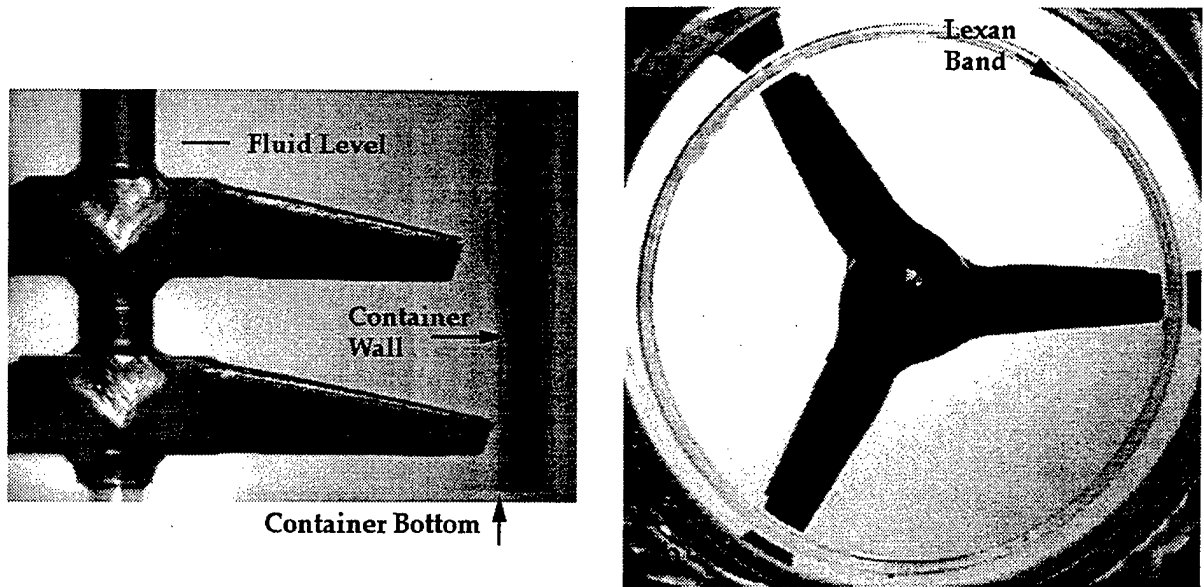


Figure 2.1. (a) Elevation and (b) Plan Views of Mixer Apparatus

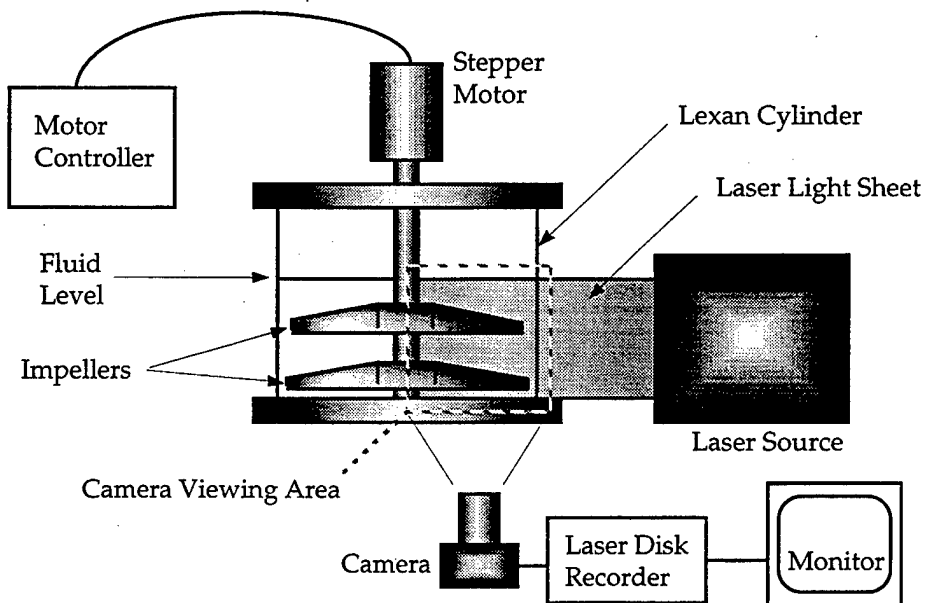


Figure 2.2. Schematic of Experimental Apparatus

The laser used was a pulsed Nd:YLF diode laser from Quantronix, Inc., operating at 527 nm. Appropriate quantities of fluorescent dye were applied to the liquid-air interface so the mixing process could be observed. The dye was essentially a passive tracer similar to any specie entraining into the liquid from the interface. The advantage of using laser light sheet visualization in combination with fluorescent dye was that we could obtain localized information on the concentration distribution as a function of mixing time and rotation rate.

2.2 Fluid Properties

To understand better the effect of fluid rheology on the migration in the extractor, both Newtonian and non-Newtonian fluids were used in these experiments. These fluids were glycerin and 0.1% by weight of aqueous Carbopol® 980 solution. Glycerin behaves as a Newtonian fluid with a viscosity of 1 Pa/s (10^3 cP). The rheology of the Carbopol solution was found to be yield-pseudoplastic and well represented by the Herschel-Bulkley model. The rheogram for this fluid is given in Figure 2.3. For shear rates less than 10 s^{-1} , the shear stress (T) can be approximated by the curve fit shown in Figure 2.3. Based on the best-fit results, the yield stress of this fluid was found to be 2.75 Pa, and the consistency factor and behavior index were 2.5 and 0.6, respectively.

2.3 Test Matrix

The current maximum rotational speed used for mixing in hot cell procedures is 3 rpm. At 3 rpm the flow is fully laminar, and with viscous fluids, we might expect flow zones that do not communicate well with each other. Thus the testing matrix was setup to determine if viscous fluids could be mixed by impeller blades rotating at this speed. Glycerin and Carbopol were used as representative fluids of Newtonian and non-Newtonian viscous fluids for the 3 rpm tests. Tests were run for both clockwise (down pressure) and counter-clockwise (up-pressure) impeller rotations to compare the mixing effectiveness. In addition to the 3 rpm tests of glycerin and carbopol, a test was performed with 30 rpm mixing of the carbopol solution to determine whether mixing times correlated with mixing speed. These test runs are summarized in Table 2.1.

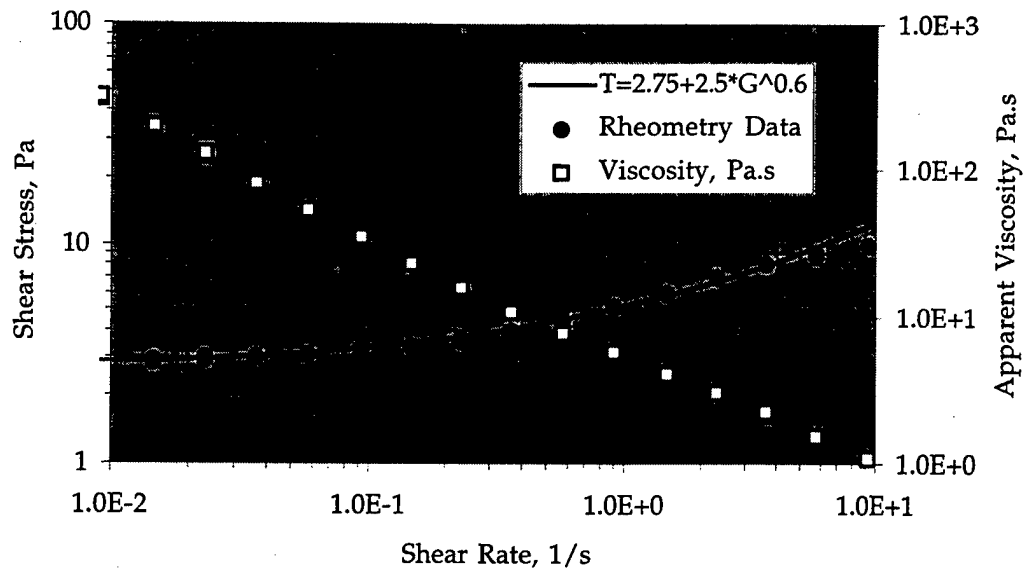


Figure 2.3. Rheogram for Working Fluid (0.1% by weight of aqueous Carbopol solution)

Table 2.1. Extractor Mixing Tests

Working Fluid	Mixing Speed (rpm)	Rotation Direction ^(a)	Comparisons Made
Glycerin	3	CCW (up pressure)	Mixing effectiveness by blade direction
"	3	CW (down pressure)	
Carbopol Solution	3	CCW (up pressure)	1. Newtonian versus non-Newtonian 2. Blade direction 3. Mixing speed
"	3	CW (down pressure)	
"	30	CW (down pressure)	

(a) CCW = counter-clockwise; CW = clockwise.

2.4 Experimental Test Results

Two sets of tests were performed, Newtonian and non-Newtonian. The Newtonian fluid is considered to be representative of the supernatant liquid and some of the salt slurries from single-shell tanks. The particular non-Newtonian rheology was selected because it closely resembles sludges in double-shell tanks (see, for example, Onishi et al. 1996 or Stewart et al. 1996).

2.4.1 Newtonian Fluid

Results of the 3-rpm, counter-clockwise rotation (up pressure) impeller mixing of glycerin are shown in Figure 2.4. Within a few minutes the fluorescing dye particles on the surface had migrated into three pockets at a mid-radius on the surface midway between the blades. A ring of dye accumulated on the surface at the wall. After 10 minutes of mixing, the pockets of dye midway between the blades had been drawn into vortices from the surface to the center of the vessel. Figure 2.4a shows one such vortex at 10 minutes. As is shown in Figure 2.5b, after 30 minutes of mixing the vortices were less pronounced, and a dye-free (clear) region began to show at the outer wall. After one hour of mixing the vortices had dissipated, but the clear region near the wall was still present, as shown in Figure 2.4c. After six hours of mixing, shown in Figure 2.4d, the dye pockets and ring at the surface were still present, and the fluid was not fully mixed.

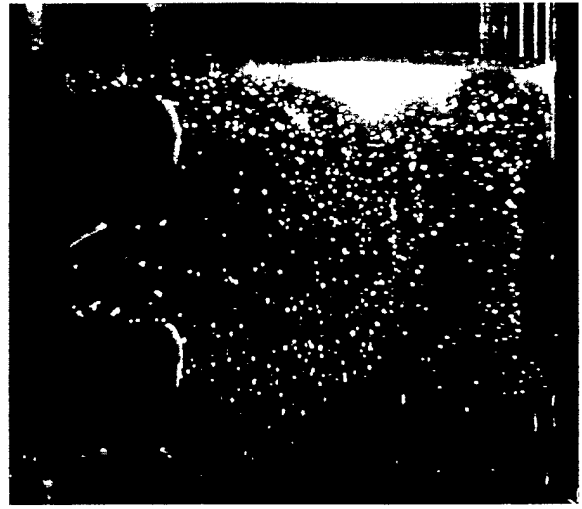
Results of the 3-rpm clockwise rotation (down pressure) impeller mixing of glycerin are shown in Figure 2.5. The fluorescing dye was more fluid in this test but retained its passive nature. The results were quite different from the up-pressure mixing; within a few minutes the dye on the surface was seen moving outward on the surface and down into the fluid at a radius near the tip of the upper blade, not reaching the outer wall. Figure 2.5a shows that after 10 minutes of stirring the dye had migrated to roughly midlevel in the fluid and was moving radially inward. The clear region at the outer wall indicates an upward flow. The combination of inward radial motion at the midlevel and clear region at the outer wall indicate upper and lower regions of circulation. As seen in Figure 2.5b, after 30 minutes of mixing the dye had circulated throughout the fluid volume except for a clear region centered on the upper blade tips. Visible in Figure 2.5b are horizontally oriented flow features near the upper blade path that indicate faster flow in the radial direction. Figure 2.5c shows the clear region at the upper blade tips present after one hour of mixing. After six hours, shown in Figure 2.5d, the glycerin and dye seem to have been homogeneously mixed.

2.4.2 Non-Newtonian Fluid

Before testing, the fluorescent dye particles were mixed with Carbopol. The dye-laden Carbopol was carefully and randomly distributed about the surface in the form of droplets (or globules) before starting the mixing motor. When mixing began, standing waves were established that moved along with the blades. The waves, due to the yield strength of the fluid, remained for the duration of mixing.



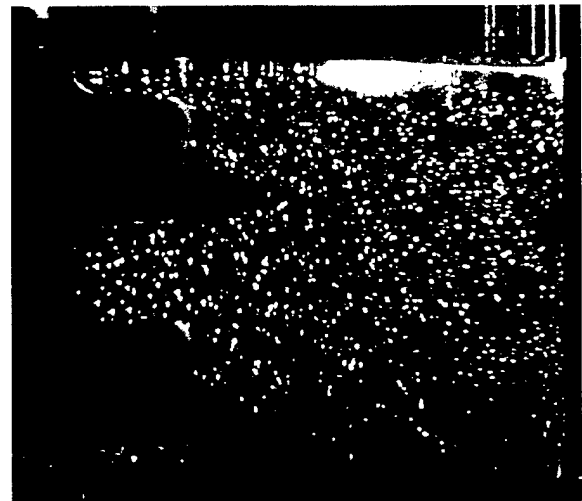
a. 10 minutes



b. 30 minutes



c. 60 minutes

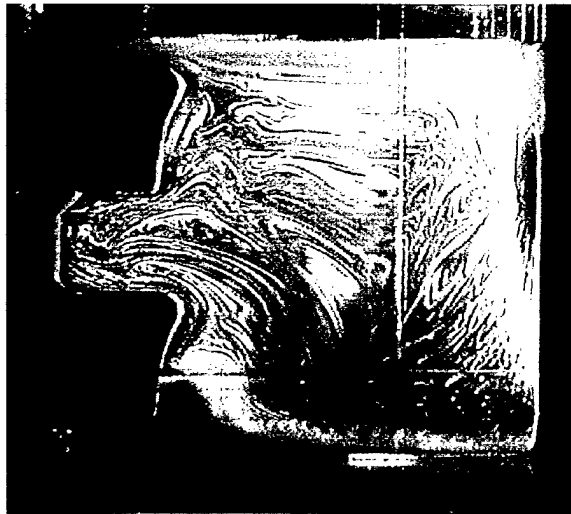


d. 6 hours

Figure 2.4. Newtonian Mixing (3-rpm, up-pressure impeller mixing of glycerin and fluorescent dye placed initially on surface)



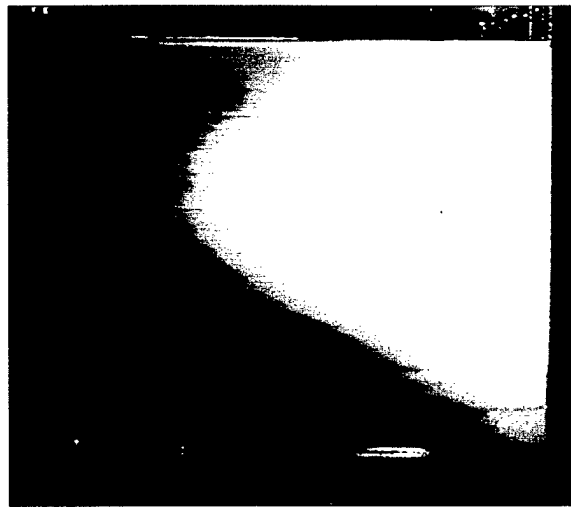
a. 10 minutes



b. 30 minutes



c. 60 minutes



d. 6 hours

Figure 2.5. Newtonian Mixing (3-rpm, down-pressure impeller mixing of glycerin and fluorescent dye placed initially on surface)

Figure 2.6 shows the results of the 3-rpm, up-pressure impeller mixing of Carbopol solution. Within a few minutes the dye was swept radially outward, and the surface was clear of virtually all dye. The dye was drawn down the outer wall and then spiraled up the impeller shaft, leaving a clear region next to the shaft, as shown in Figure 2.6a. Figure 2.6b shows the dye distribution after 30 minutes of mixing. A clear toroidal region was present at mid- to near-wall radius between the impellers, and dye began to accumulate in the form of a ring at the outer edge of the top surface. After one hour of mixing, shown in Figure 2.6c, the clear region next to the shaft was decreasing in size, but the toroidal zone was still present. After 46 hours of mixing the clear toroidal zone had vanished, but a thick ring of unmixed dye remained at the outer top surface and is visible in Figure 2.6d.

Results of the 3-rpm, down-pressure mixing of Carbopol solution are shown in Figure 2.7. The dye was drawn into narrow strands and stretched into spiral forms on the surface. After 10 minutes of mixing these strands of fluorescent dye began to spiral down the center at a radius somewhat larger than the impeller blade hubs, leaving a clear region next to the impeller shaft. This spiral flow feature is shown in Figure 2.7a. After 30 minutes of mixing, most of the dye had been drawn down from the surface along the impeller shaft and was cycling back toward the surface at the outer wall, as shown in Figure 2.7b. Figure 2.7c shows the particle distribution after one hour. By this time more dye had been pushed up the outer wall of the container, and a clear toroidal region at mid- to near-wall radius was observed between the impellers. Another feature that developed was a low particle density region at about three-quarter radius near the surface. The stagnant toroidal region was still present after 72 hours of mixing, as is shown in Figure 2.7d, but mixing appeared to be more complete in this down-pressure mixing than in the up-pressure mixing.

A fifth test was performed to observe the effect of increased rotational speed on the mixing of carbopol solution. A factor of ten times speed increase was chosen. At 30 rpm, the flow was still fully laminar.

Within two minutes of starting the motor at 30 rpm, a flow pattern developed similar to that observed at 3 rpm. As shown in Figure 2.8a, The particles had been drawn down near the shaft and were being pushed up the outer wall, leaving a particle-free toroidal region. This flow pattern is more pronounced in Figure 2.8b at 3 minutes and is similar to the 3 rpm case at 30 minutes (Figure 2.7b). Figure 2.8c shows the flow pattern after 6 minutes (similar to 1 hour at 3 rpm).



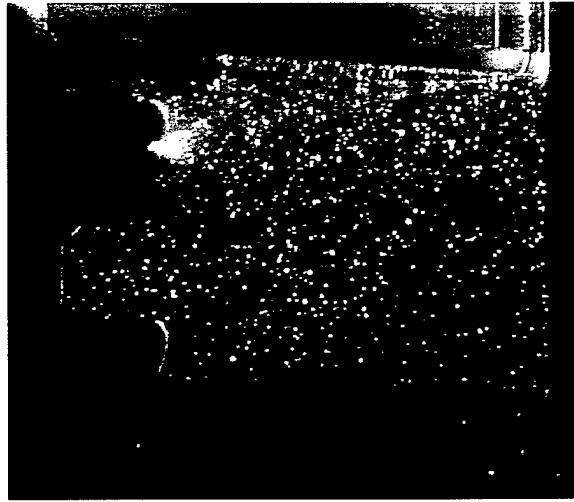
a. 10 minutes



b. 30 minutes



c. 60 minutes



d. 46 hours

Figure 2.6. Non-Newtonian Mixing (3-rpm, up-pressure impeller mixing of Carbopol solution and fluorescent dye placed initially on surface)

Particles had circled a clear toroidal region several times, folding each subsequent path inside the last. Figure 2.8c also shows a low particle density region at about $3/4$ radius near the surface, similar to the 3-rpm case. Figure 2.8d is a photograph taken after 4-1/2 hours of mixing. Surface particle density had been depleted, and mixing seemed to be occurring on a very short scale only. Clear zones were still present, similar to the 3-rpm case for comparable impeller revolutions, indicating that the laminar mixing time was correlated to mixing speed.



a. 10 minutes



b. 30 minutes



c. 60 minutes

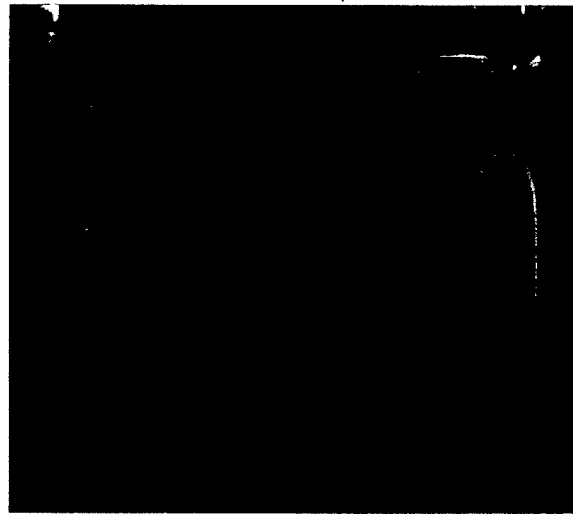


d. 72 hours

Figure 2.7. Non-Newtonian Mixing (3-rpm, down-pressure impeller mixing of Carbopol solution and fluorescent dye placed initially on surface)



a. 2 minutes



b. 3 minutes



c. 6 minutes



d. 4.5 hours

Figure 2.8. Non-Newtonian Mixing (30-rpm, down-pressure impeller mixing of Carbopol and fluorescent dye placed initially on surface)

3.0 Computational Method

The objective of the computer modeling was to develop a tool for parametric analysis of the extractor mixing process. Development of the model described in this section began prior to the mixing tests. Model development and validation by comparison with experimental results would enable simulations of the mixing process for a range of fluid properties and mixing speeds. Simulating the extractor mixing system poses a serious challenge for computer codes due to the complex geometry, the presence of rotating mixer blades, the non-Newtonian fluid behavior, and multiple fluid phases. The CFX-F3D computer code was chosen for the task of simulating the mixing process because it has capabilities for dealing with these challenges.

3.1 CFX-F3D Model

Figure 3.1 represents elevation and plan views of the 3-dimensional CFX-F3D model developed for the computations. The model contained 23 radial cells, 35 axial cells, and 48 azimuthal cells. No-slip boundary conditions existed at the bottom and outer wall of the vessel. The no-slip condition was also imposed at the impeller blades and shaft, which both rotated at 3 rpm in either direction. The free surface interface was not modeled, but fluid at the surface was

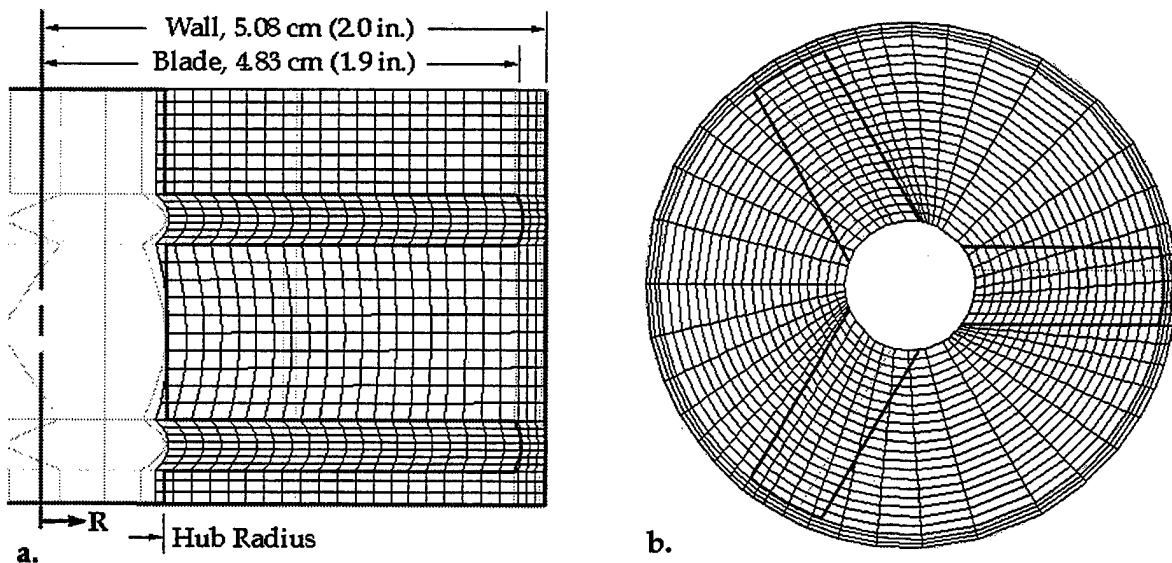


Figure 3.1. Elevation and Plan Views of Mixer Model Domain

allowed to move with full slip. Several simplifications were made to the model geometry. The impeller blades were given a constant 24-in. pitch and constant, average chord length of 1.207 cm (0.475 in.). Both impellers were made an equal radius of 4.83 cm (1.9 in.), and the impeller shaft was made a constant diameter equal to the impeller blade hub (2.54 cm [1.0 in.]). The sealing ring at the mixer bottom was not represented in the model to reduce its complexity.

3.2 Computations

Respective fluid properties of glycerin and Carbopol solution were used in the computations, including a constant viscosity for the glycerin and Herschel-Bulkley rheology model for the Carbopol. A brief simulation was run to test the rotating coordinate system and boundary conditions. When it was determined that the mixer rotation was correct and the flow field showed that the boundary conditions were correctly imposed, a second fluid phase (with properties identical to the base fluid) was added to the model to represent the fluorescent dye (or passive tracer) transported through the base fluid in the mixing experiments. In the computations the uppermost three planes of cells were initialized with 1% by volume of the second phase. Placement of the tracer near the model fluid surface was arbitrary due to the random, nonuniform placement of the tracer in the experiments.

3.2.1 Newtonian Fluid Simulations

In early attempts to simulate mixing of glycerin and fluorescent dye, the tracer was modeled as a continuous fluid phase. This so-called "homogeneous" model assumed that the flow solution for each phase was identical except for the volume fractions, which were determined by solving separate continuity equations for each phase. With the homogeneous model, interphase mixing was artificially favorable, and the code predicted very short mixing times. Figure 3.2 presents results of a run simulating 400 seconds of 3-rpm glycerin mixing using the homogeneous model. The figure represents a slice through the data in a plane similar to the laser light sheet of the experiments and gives volume concentration of the tracer. High tracer concentration is red, and low concentration is violet. The figure shows that the code predicted considerable mixing within the first 400 seconds. This figure should be similar in appearance to Figure 2.5a.

Some experimentation was required with the CFX-F3D multiphase models before similar mixing features began to emerge in the laboratory tests and computations. Determining the most suitable multiphase model was complicated by the wait time to obtain simulation results; with the homogeneous model, 16 hours were required on an IBM 590 workstation to simulate the first 400 seconds of mixing. A multiphase model was tested that treated the tracer as a disperse solid phase

within the base fluid. The “disperse” phase model solved separate momentum and continuity equations for each phase. The disperse phase was defined as solid particles of 50 micron diameter, and a standard drag curve was used to determine the momentum transfer to the particles.

Figure 3.3 presents results of a run simulating 400 seconds of 3 rpm glycerin mixing with the disperse model. The disperse model predicted much less mixing and exhibited features similar to those observed in the experiments; features of Figure 3.3 are roughly comparable to those of Figure 2.5a. The tracer moved down into the fluid at a radius near the tip of the upper blade, not reaching the outer wall. At the midlevel, concentration gradients moved inward radially, and a clear region existed at the outer wall. The high concentration of tracer on the surface at the outer wall was a remnant of the initial condition. The disperse phase model was computationally intensive, requiring six times more computer time than the homogeneous model (97 hours of CPU time for 400 seconds of simulated mixing). Despite the longer computational times, the disperse model was used in favor of the homogeneous model for the remaining computations due to improved mixing predictions.

3.2.2 Non-Newtonian Fluid Simulations

Figure 3.4 presents results of a run simulating 400 seconds of 3-rpm, down-pressure Carbopol mixing. The results show less mixing of the tracer into the base fluid than in the Newtonian case but similar mixing features. The main feature observed early in the non-Newtonian mixing experiment was the tracer spiraling down the center at a radius somewhat larger than the impeller blade hubs, as in Figure 2.5b. This feature was not reproduced in the simulation. Instead, the tracer moved down into the fluid near the blade tip radius as in the Newtonian experiment and simulation.

Figure 3.5 represents the tracer concentration in Carbopol after 400 seconds of simulated, 3-rpm, up-pressure mixing. Similar to the experiment, tracer concentration was very low at the center of the domain, and the tracer was being moved outward and down the container wall. Unlike the experiment, the tracer was not spiraled through the model domain. This difference is to be expected in the computational model which does not have the grid resolution to capture such features. Other differences between the simulations and tests of Carbopol mixing may be attributable in part to the absence of a free surface, and hence the standing wave, in the model. Absence of the sealing ring might also affect the flow field. Another potential reason for differences is that the Herschel-Bulkley model in the code may not accurately simulate the fluid yield stress. Further model development would likely yield a more suitable model for a parametric study; this might include a Lagrangian particle tracking model that is available in the CFX-F3D code. This Lagrangian model was not used in this work due to project scope and time constraints.

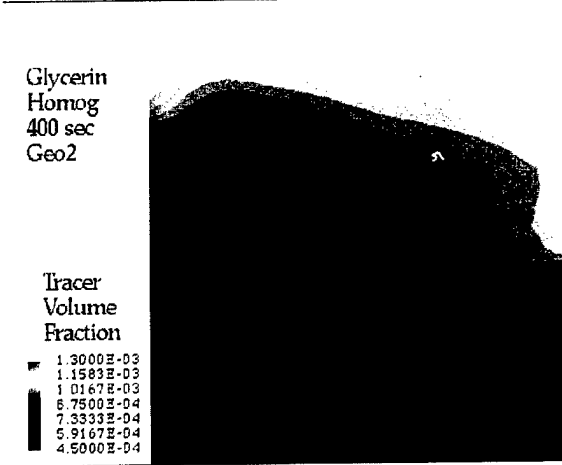


Figure 3.2. Tracer in Glycerin after 400 Seconds of 3-rpm, Down-Pressure Mixing (homogeneous multiphase model)

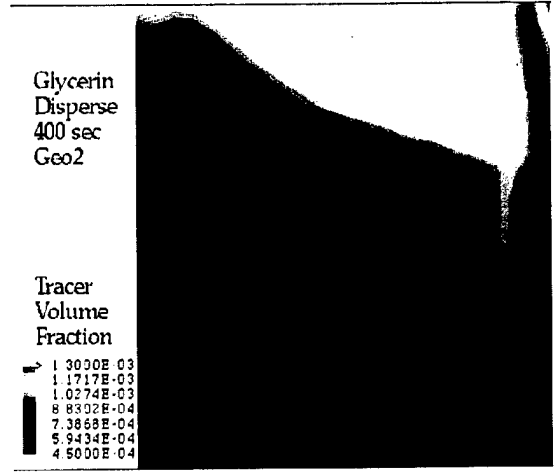


Figure 3.3. Tracer in Glycerin after 400 Seconds of 3-rpm, Down-Pressure Mixing (disperse multiphase model)

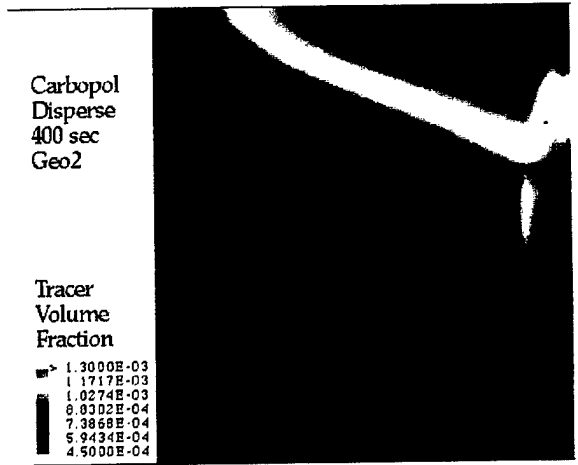


Figure 3.4. Tracer in Carbopol Solution after 400 Seconds of 3-rpm, Down-Pressure Mixing (disperse multiphase model)

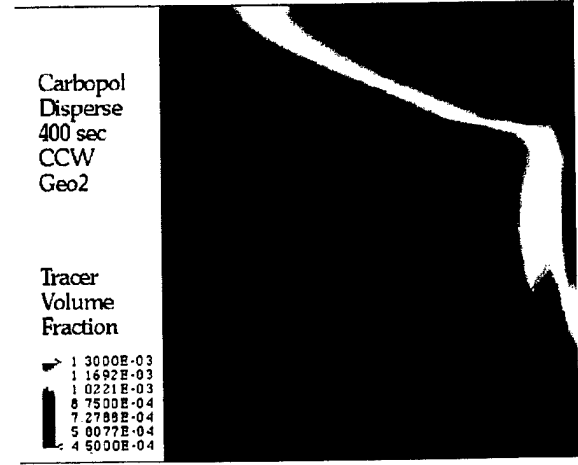


Figure 3.5. Tracer in Carbopol Solution after 400 Seconds of 3-rpm, Up-Pressure Mixing (disperse multiphase model)

4.0 Conclusions

Tests have been performed to examine the effectiveness of the RGS extractor at mixing Newtonian and non-Newtonian fluids. The tests demonstrated that rotational direction of the pitched impeller blades was not a determining factor in mixing time. Fluid rheology, however, was a factor; the Newtonian fluid required at least six hours to mix at 3 rpm, and the non-Newtonian fluid required at least 46 hours at 3 rpm to become mostly mixed. While the tests demonstrated that in a non-Newtonian fluid a tracer would be transported in a cycle from the surface through the volume and back to the surface within several minutes, there were stagnant regions within the fluid that required days to be mixed. A 30-rpm mixing test demonstrated that the laminar mixing time of the non-Newtonian fluid was correlated to the mixing speed. Turbulence would be required to achieve mixing times on the order of minutes, and transition to turbulence with the current extractor configuration is not likely to be achieved. These tests have demonstrated that with the current configuration of the RGS extractor, complete mixing of the waste samples should not be expected within the hot-cell operating procedure.

The CFX-F3D simulation of Newtonian fluid mixing gave results comparable to the tests while simulation of non-Newtonian fluid mixing would require further development. The original intent of the computer models was to allow parametric study of the mixing process. In light of the laboratory test results, detailed parametric analysis of the mixing process was not performed.

5.0 References

- Bobroff S, RJ Phillips, and A Shekarriz. 1997. *Nuclear Magnetic Resonance Measurement of Ammonia Diffusion in Dense Solid-Liquid Slurries*. PNNL-11678, Pacific Northwest National Laboratory, Richland, Washington.
- Distelhoff MFW, AJ Marquis, JM Nouri, and JH Whitelaw. 1997. "Scalar Mixing Measurements in Batch Operated Stirred Tanks." *Canadian Journal of Chemical Engineering*, 75:641-652.
- Fox EA and VE Gex. 1956. "Single-Phase Blending of Liquids." *AIChE J.* 2(4):539-54
- Mahoney LA, ZI Antoniak, and JM Bates. 1997. *Composition and Quantities of Retained Gas Measured in Hanford Waste Tanks 241-U-103, S-106, BY-101, and BY-109*. PNNL-11777, Pacific Northwest National Laboratory, Richland, Washington.
- Moo-Young M, K Tichtar, and FAL Dullien. 1972. "The Blending Efficiencies of Some Impellers in Batch Mixing." *AIChE J.* 18:178-182.
- Onishi Y, R Shekarriz, KP Recknagle, PA Smith, J Liu, YL Chen, DR Rector, and JD Hudson. 1996. *Tank SY-102 Waste Retrieval Assessment: Rheological Measurements and Pump Jet Mixing Simulations*. PNNL-11352, Pacific Northwest National Laboratory, Richland, Washington.
- Shekarriz A, DR Rector, LA Mahoney, MA Chieda, JM Bates, RE Bauer, NS Cannon, BE Hey, CG Linschooten, FJ Reitz, and ER Siciliano. 1997. *Composition and Quantities of Retained Gas Measured in Hanford Waste Tanks 241-AW-101, A-101, AN-105, AN-104, and AN-103*. PNNL-11450 Rev. 1, Pacific Northwest National Laboratory, Richland, Washington.
- Stewart CW, JM Alzheimer, ME Brewster, G Chen, RE Mendoza, HC Reid, CL Shepard, and G Terrones. 1996. *In Situ Rheology and Gas Volume in Hanford Double-Shell Waste Tanks*. PNNL-11296, Pacific Northwest National Laboratory, Richland, Washington.

Distribution

<u>No. of Copies</u>		<u>No. of Copies</u>	
Offsite		2	<u>SESC</u>
2	Office of Scientific and Technical Information	NS Cannon DB Graves	L6-38 L6-38
Onsite		28	<u>Pacific Northwest National Laboratory</u>
1	<u>DOE Richland Operations Office</u>	JM Bates (5) SQ Bennett	K7-15 K7-90
	CA Groendyke S7-54	JW Brothers (5) BC Bunker	K9-20 K8-93
4	<u>Duke Engineering Services Hanford</u>	JA Fort SD Colson	K7-15 K8-88
	RE Bauer (3) S7-14	CW Stewart	K7-15
	GD Johnson S7-14	LA Mahoney	K7-15
		LR Pederson	K2-44
2	<u>Numatec Hanford Company</u>	KP Recknagle (5)	K7-15
	BE Hey T6-07	A Shekarriz	K7-15
	JC Person T6-07	Information Release (5)	K1-06

M98051303



Report Number (14) PNNL--11759

Publ. Date (11) 1997 11
Sponsor Code (18) ~~EM~~ DOE/EM, XF
UC Category (19) UC-2030, DOE/ER

DOE